

Mixed convection from an arbitrarily inclined semi-infinite flat plate—II. The influence of the Prandtl number

G. WICKERN†

Institut für Thermo- und Fluidodynamik, Ruhr-Universität, Bochum, F.R.G.

(Received 14 September 1989)

Abstract—The effect of the Prandtl number on laminar boundary layer flow over an arbitrarily inclined semi-infinite flat plate, either heated or cooled, is studied. The interaction between the buoyancy forces and the basic forced convection flow is determined. The effect of the inclination angle has already been discussed in Part I. It turned out that investigating the horizontal and the vertical plate, respectively, provides enough information to understand the flow at arbitrarily inclined plates. Thus in Part II the influence of the Prandtl number will be demonstrated extensively for the horizontal and the vertical plate only. The Prandtl number dependence of the flow and heat-transfer characteristics is first investigated by asymptotic expansions for $Pr \rightarrow 0$ and $Pr \rightarrow \infty$. In addition numerical solutions are given for a variety of finite Prandtl numbers. The results are compared with those from the asymptotic theory.

1. INTRODUCTION

A DETAILED discussion of how buoyancy forces affect the flow over inclined plates is given in Part I. This second part focuses on the effect of the Prandtl number on this kind of mixed convection flows. Although the asymptotic theories for small and high Prandtl numbers are well known for pure forced convection flows, little has been done to extend them to mixed convection flows. Solutions have been given so far only for asymptotically small buoyancy forces, see for example Hieber [1] for mixed convection at the horizontal plate. On the other hand, numerical solutions with finite buoyancy parameters are given only for the Prandtl-number range 0.1–10 (see for example refs. [2–6]). In this paper numerical solutions will be given for finite buoyancy parameters at infinitely small and high Prandtl numbers at horizontal and vertical plates, respectively. In Part I it was demonstrated how the qualitative behaviour of mixed convection flows over arbitrarily inclined plates can be derived from the two extreme orientations in space (vertical and horizontal). In addition, numerical solutions for finite Prandtl numbers in the range 0.01–100 were calculated and compared with the asymptotic solutions for $Pr \rightarrow 0$ and $Pr \rightarrow \infty$.

With the help of the asymptotic solutions the complicated interaction between the thermal and velocity boundary layer can be analysed quite clearly. With the appropriate scalings of the different layers, numerical problems are avoided for the extreme Prandtl numbers. Finally, applying the asymptotic theory, a solution can be given for any extreme Prandtl number

when the basic solution has been found (often the asymptotic solution can also be extended to moderate values of Pr). Therefore, the asymptotic solutions are the basis for correlations covering the whole range of Prandtl numbers (see Churchill and Usagi [7]). The subsequent discussion of the Pr dependence of mixed convection results, given in the following, is based mainly on the asymptotic approach.

An additional benefit of the asymptotic theory was found in the adverse buoyancy case at the horizontal plate. Numerical problems, reported in Part I (detailed in ref. [8]) for the horizontal plate, are completely eliminated in the asymptotic limit $Pr \rightarrow 0$. The mutual coupling between velocity and thermal boundary layer is avoided in the asymptotic approach. Thus the interaction mechanism is much simpler and the solution in the vicinity of separation can be calculated without any problems.

2. BASIC EQUATIONS

The problem under consideration is shown in Fig. 1. The equations that follow are valid for any inclination angle α , although numerical solutions will be given for vertical and horizontal plates only ($\alpha = 0^\circ, 90^\circ, 180^\circ, 270^\circ, \dots$). The basic equations are (see equations (8)–(11) in Part I)

$$f''' + \frac{1}{2}ff'' = -x_s^{(2+2e)/(1+2e)} \frac{Gr}{Re^2} \sin \alpha \vartheta - \frac{1}{2}\eta_s x_s \frac{Gr}{Re^{5/2}} \times \cos \alpha \vartheta + x_s \left(\frac{1}{2} + e \right) \left(\frac{\partial p}{\partial x_s} + f' \frac{\partial f'}{\partial x_s} - \frac{\partial f}{\partial x_s} f'' \right) \quad (1)$$

$$p' = x_s \frac{Gr}{Re^{5/2}} \cos \alpha \vartheta \quad (2)$$

† Present address: Mercedes-Benz AG, 7032 Sindelfingen, Postfach 226, F.R.G.

NOMENCLATURE

c_f friction coefficient, equation (10)
 c_p specific heat
 e exponent of temperature distribution, see Part I
 f scaled streamfunction, see Part I
 \bar{g} scaled pressure, equation (23)
 g^* gravitational acceleration
 Gr Grashof number
 $\hat{G}r$ modified Grashof number for $\dot{q}_w = \text{const.}$, equation (7)
 L^* reference length
 Nu Nusselt number, equation (11)
 p pressure
 Pe Peclet number, $Re \cdot Pr$
 Pr Prandtl number
 \dot{q}_w wall heat flux
 Re Reynolds number
 T temperature
 U_∞ free stream velocity
 x, y coordinate system
 x_s, η_s scaled coordinate system for velocity boundary layer, see Part I.

β coefficient of thermal expansion
 δ boundary layer thickness
 η dynamic viscosity
 η_T scaled y-coordinate for thermal boundary layer, equation (12)
 ϑ reduced dimensionless temperature, see Part I
 λ thermal conductivity
 ρ density
 τ_w wall shear stress.

Subscripts

i, o inner, outer
 s scaled for the velocity boundary layer
 T scaled for the thermal boundary layer
 w wall value
 x local quantity
 ∞ free stream value.

Superscripts

* dimensional quantity
 ' derivative with respect to η_s
 $\dot{}$ derivative with respect to η_T
 $\hat{}$ modified for $\dot{q}_w = \text{const.}$
 $\bar{}$ scaled quantity.

Greek symbols

α inclination angle to the horizontal

$$\vartheta'' + \frac{1}{2}Pr f \vartheta' - e Pr f' \vartheta = Pr x_s (\frac{1}{2} + e) \left[f' \frac{\partial \vartheta}{\partial x_s} - \frac{\partial f}{\partial x_s} \vartheta' \right] \quad (3)$$

with the associated boundary conditions

$$\left. \begin{aligned} f(x_s, 0) = 0, & \quad \vartheta(x_s, 0) = 1 & T_w = \text{const.} \\ f'(x_s, 0) = 0, & \quad \vartheta(0, 0) = 1 \\ f'(x_s, \infty) = 1, & \quad \vartheta'(x_s, 0) = \vartheta'(0, 0) \\ p(x_s, \infty) = 0, & \quad \vartheta(x_s, \infty) = 0. \end{aligned} \right\} q_w = \text{const.} \quad (4)$$

For details of the nondimensionalization see Part I; a prime denotes partial differentiation with respect to η_s .

The set of equations (1)–(4) can either be treated numerically to obtain solutions for finite Prandtl num-

bers or it can be subject to an asymptotic analysis with respect to the Prandtl number ($Pr \rightarrow 0$ and $Pr \rightarrow \infty$). The length scale L^* , which is purely formal, can be eliminated. Thus the number of independent parameters is reduced by one (as already demonstrated in Part I). This leads to modified buoyancy parameters (which are actually only used for representation of the results)

$$\frac{Gr_x}{Re_x^2} \sin \alpha = x_s^{1+e} \frac{Gr}{Re^2} \sin \alpha \quad (5)$$

$$\frac{Gr_x}{Re_x^{5/2}} \cos \alpha = x_s^{1/2+e} \frac{Gr}{Re^{5/2}} \cos \alpha \quad (6)$$

Now the solutions at the wall are only a function of these two local buoyancy parameters, the Prandtl number and the exponent of the temperature distribution.

For the constant surface heat flux case this representation is still inadequate, since there is no well-defined temperature difference to form a suitable Grashof number. Thus a modified Grashof number is introduced for the constant heat flux case

$$\hat{G}r_x \equiv \frac{\beta^* \dot{q}_w^* g^* x^{*4} \rho_\infty^{*2}}{\lambda_\infty^* \eta_\infty^{*2}} \quad (7)$$

The adequate buoyancy parameters for the constant surface heat flux case are then

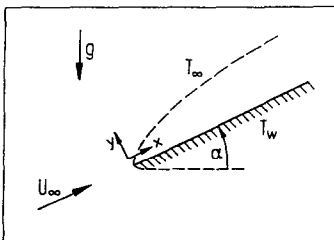


FIG. 1. The coordinate system for mixed convection from an arbitrarily inclined flat plate.

$$\frac{\hat{G}r_x}{Re_x^{5/2}} \sin \alpha = x_s^{1+e} \frac{Gr}{Re^2} \sin \alpha (-\vartheta'(0, 0)) \quad (8)$$

$$\frac{\hat{G}r_x}{Re_x^3} \cos \alpha = x_s^{1/2+e} \frac{Gr}{Re^{5/2}} \cos \alpha (-\vartheta'(0, 0)) \quad (9)$$

(with $e = \frac{1}{2}$ for $\dot{q}_w = \text{const.}$).

With these definitions the buoyancy parameters in equations (1)–(4) can be related to known quantities for the constant heat flux case.

The numerical results in terms of dimensionless quantities are the local skin friction coefficient c_{fx} and the local Nusselt number

$$c_{fx} = \frac{\tau_w^*}{\rho_\infty^* U_\infty^{*2}} \quad (10)$$

$$Nu_x = \frac{\dot{q}_w^* x^*}{\lambda_\infty^* (T_{w\infty} - T_\infty)} \quad (11)$$

(c_{fx} has the index x to be consistent with Part I).

In cases where partial differential equations had to be solved a Keller box scheme was employed. The typical resolution in the y -direction was 130 grid-points. The ordinary differential equations obtained from the asymptotic approach were treated by a fourth-order Runge–Kutta scheme.

3. ASYMPTOTIC THEORY FOR SMALL PRANDTL NUMBERS

Figure 2 shows the flow field and the temperature distribution for forced convection in a low Prandtl number fluid. The transport mechanism for thermal energy is much more effective than that for momentum. As a consequence the thermal boundary is much thicker than the velocity boundary. That is why deviations of the velocity profile from the uniform main stream velocity are higher order effects in an asymptotic approach to the heat transfer problem. This is no longer true for cases, where considerable buoyancy forces exist. The correct asymptotic description then has to be derived by formal expansions and matching between an inner and an outer layer.

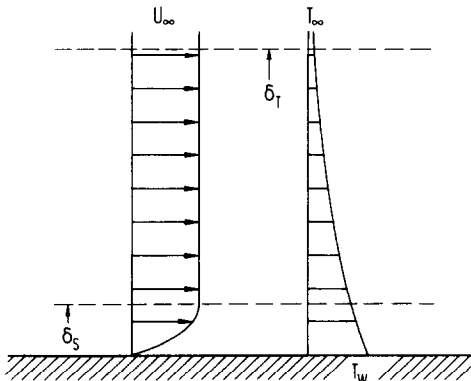


FIG. 2. Sketch of the scaling of velocity and thermal boundary layer for small Prandtl numbers.

For $Pr \rightarrow 0$ the scaling of the velocity boundary layer is no longer appropriate for the thermal boundary layer. A new y -coordinate scaled by the Prandtl number and a suitable scaled streamfunction must be introduced

$$\eta_T = Pr^{1/2} \eta_s \quad (12)$$

$$\tilde{f} = Pr^{1/2} f. \quad (13)$$

Since the thermal boundary layer is much thicker than the velocity boundary layer, it can be regarded as the outer layer of a matched asymptotic expansion. The equations for the inner layer are obtained from the original set of equations (equations (1)–(4), in the original coordinate η_s) by setting Pr to zero

$$f''' + \frac{1}{2}ff'' = -x_s^{(2+2e)/(1+2e)} \frac{Gr}{Re^2} \sin \alpha \vartheta + (\frac{1}{2}+e)x_s \left(\frac{\partial p}{\partial x_s} + f' \frac{\partial f'}{\partial x_s} - \frac{\partial f}{\partial x_s} f'' \right) \quad (14)$$

$$p' = 0 \quad (15)$$

$$\vartheta' = 0 \quad (16)$$

(with $e = 0$ for $T_w = \text{const.}$ and $e = \frac{1}{2}$ for $\dot{q}_w = \text{const.}$). The equations for the outer layer (the thermal boundary layer, in the new coordinate η_T) are

$$\frac{1}{2}\tilde{f}\tilde{f}' = -x^{(2+2e)/(1+2e)} \frac{Gr}{Re^2} \sin \alpha \vartheta - \frac{1}{2}\eta_T x_s \frac{Gr}{Re^{5/2}} \cos \alpha Pr^{-1/2} \vartheta + (\frac{1}{2}+e)x_s \left(\frac{\partial p}{\partial x_s} + \tilde{f}' \frac{\partial \tilde{f}'}{\partial x_s} - \frac{\partial \tilde{f}}{\partial x_s} \tilde{f}'' \right) \quad (17)$$

$$p' = x_s \frac{Gr}{Re^{5/2}} \cos \alpha Pr^{-1/2} \vartheta \quad (18)$$

$$\vartheta'' + \frac{1}{2}\tilde{f}\vartheta' - e\tilde{f}'\vartheta = (2+e)x_s \left[f' \frac{\partial \vartheta}{\partial x_s} - \frac{\partial f}{\partial x_s} \vartheta' \right] \quad (19)$$

(dots denote partial differentiation with respect to η_T).

The two layers are coupled by matching conditions, which supply a suitable number of additional boundary conditions to complete the closure of the problem :

inner layer

$$\begin{aligned} f_i(x_s, 0) &= 0 \\ f_i'(x_s, 0) &= 0 \\ f_i'(x_s, \infty) &= p_o(x_s, 0) \\ \vartheta_i(x_s, 0) &= 1 \quad (T_w = \text{const.}) \end{aligned}$$

or

$$\begin{aligned} \vartheta'_i(x_s, 0) &= 0 \quad (\dot{q}_w = \text{const.}) \\ \vartheta'_i(x_s, \infty) &= \vartheta'_o(x_s, 0) \end{aligned} \quad (20)$$

outer layer

$$\begin{aligned} \bar{f}'_o(x_s, 0) &= 0 \\ \bar{f}'_o(x_s, \infty) &= 1 \\ p_o(x_s, \infty) &= 0 \\ \vartheta_o(x_s, 0) &= 1 \quad (T_w = \text{const.}) \end{aligned}$$

or

$$\left. \begin{aligned} \vartheta_o(0, 0) &= 1 \\ \vartheta'_o(x_s, 0) &= \vartheta'_o(0, 0) \end{aligned} \right\} (\dot{q}_w = \text{const.}) \\ \vartheta_o(x_s, \infty) &= 0. \quad (21)$$

The coupling is in one direction only, since the complete outer layer can be calculated without knowledge of the inner layer, whereas the solution of the outer layer is part of the boundary conditions for the inner layer. This scheme fails when separation occurs in the inner layer and a square root singularity appears. Although the solution of the outer layer can be extended arbitrarily beyond this point, it is invalid since then the premises underlying the formal expansion are violated. This unidirectional coupling is the explanation for the behaviour of the heat transfer characteristics in the vicinity of separation, which for $Pr \rightarrow 0$ is not affected by separation. The temperature gradient at the wall is determined by the outer layer without a mechanism of information transfer through the inner part of the boundary layer.

The buoyancy force driving the flow on vertical plates is associated with $\sin \alpha$ and will be denoted as 'direct free convection'. The flow mechanism for free convection from a horizontal plate is completely different. The flow direction is normal to the gravity vector and fluid motion is possible only due to an induced pressure gradient. Buoyancy is proportional to $\cos \alpha$ then, and the resulting flow is called 'indirect free convection'. For a detailed discussion of the two kinds of buoyancy forces driving the flow on inclined plates the reader is referred to Part I. As demonstrated there, the flow over arbitrarily inclined plates can be characterized by studying vertical and horizontal plates alone.

Results for small Prandtl numbers are shown in Figs. 3(a)–(d) for mixed convection from a vertical plate, and in Figs. 4(a)–(d) for mixed convection from a horizontal plate. Generally it can be stated that, if there is only a weak dependence on the Prandtl number, the results are shown in terms of the original dimensionless variables, and the influence of Pr can be seen from the different graphs in the plots of numerical results. If there is a strong dependence, the original variables have to be rescaled by the Prandtl number, and only a secondary influence of Pr can be seen in the plots. This is the case for the Nusselt number,

which is now given in terms of the Peclet number ($Pe = Re \cdot Pr$). The lower the Prandtl number, the thicker the thermal boundary layer and the stronger the buoyancy forces. Thus in the aiding case convection is enhanced for low Pr and in the opposing case flow separation is induced earlier. Due to the fact that the mechanism of indirect free convection is mainly dependent on the thermal boundary layer thickness, the buoyancy forces at the horizontal plate are much more Pr dependent than those at the vertical plate. This has to be taken into account by introducing new buoyancy parameters rescaled with the Prandtl number.

Another consequence of the unidirectional coupling is the non-existence of regular separation in the case of vanishing Prandtl numbers. As can be seen in Fig. 5, which shows the singular lines of the complete solution, the second quadrant is no longer fully accessible for $Pr \rightarrow 0$. For $Pr = O(1)$ regular separation can occur there. (For details see Part I.) Although a pressure gradient normal to the wall exists in the outer layer, the solution is not kept regular at the onset of separation in the inner layer, due to the lack of interactive coupling. Calculating the singular lines in this diagram the buoyancy parameters had to be varied independently. Thus the study was no longer confined to vertical or horizontal plates alone.

4. ASYMPTOTIC THEORY FOR LARGE PRANDTL NUMBERS

Similar to the case of small Prandtl numbers the flow regime for large Prandtl numbers has to be split into two parts, one with the scaling of the velocity boundary layer and one with the scaling of the thermal boundary layer. For large Prandtl numbers the transport of thermal energy is much weaker than the momentum transport. As a consequence the thermal boundary layer is thin compared to the velocity boundary layer. This flow situation is shown in Fig. 6.

The thermal boundary layer scaling again can be taken from the well-known forced convection case. The scalings of streamfunction and pressure are different from those of the forced convection case as a consequence of the more complex flow situation. They are

$$\bar{\eta}_T = Pr^{1/3} \eta_s \quad (22)$$

$$\bar{f} = Pr^{2/3} f$$

$$\bar{g} = Pr^{-1/3} p. \quad (23)$$

These transformations are valid for the inner layer. For the outer layer, which has ambient temperature, the basic equations are relatively unaffected. Without buoyancy terms, they reduce to the well-known Blasius form. As in the low Prandtl number case, the two sets of equations (for the inner and the outer layer) are derived from the basic equations now with the Prandtl number going to infinity. The partial

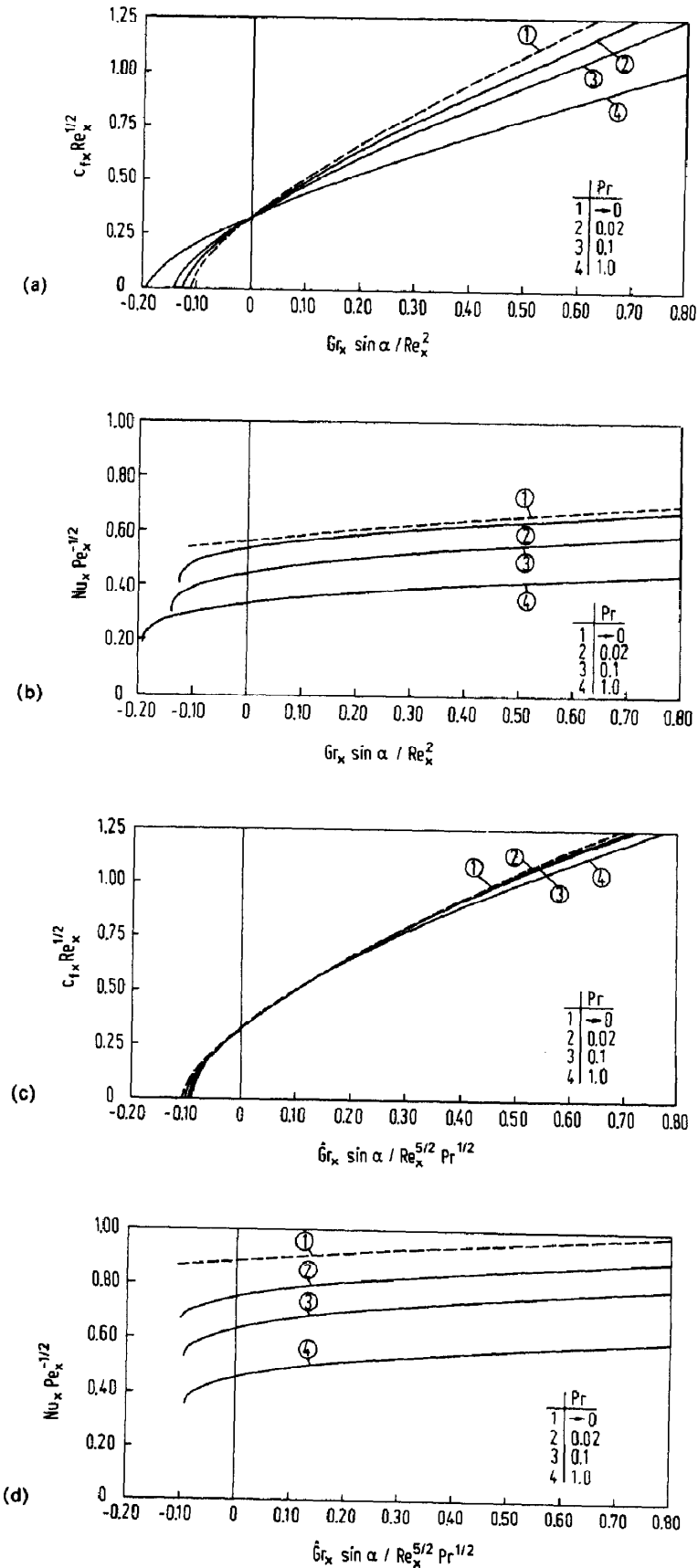


FIG. 3. Friction coefficient and Nusselt number for mixed convection from a vertical flat plate for small Prandtl numbers: (a), (b) constant wall temperature; (c), (d) constant surface heat flux.

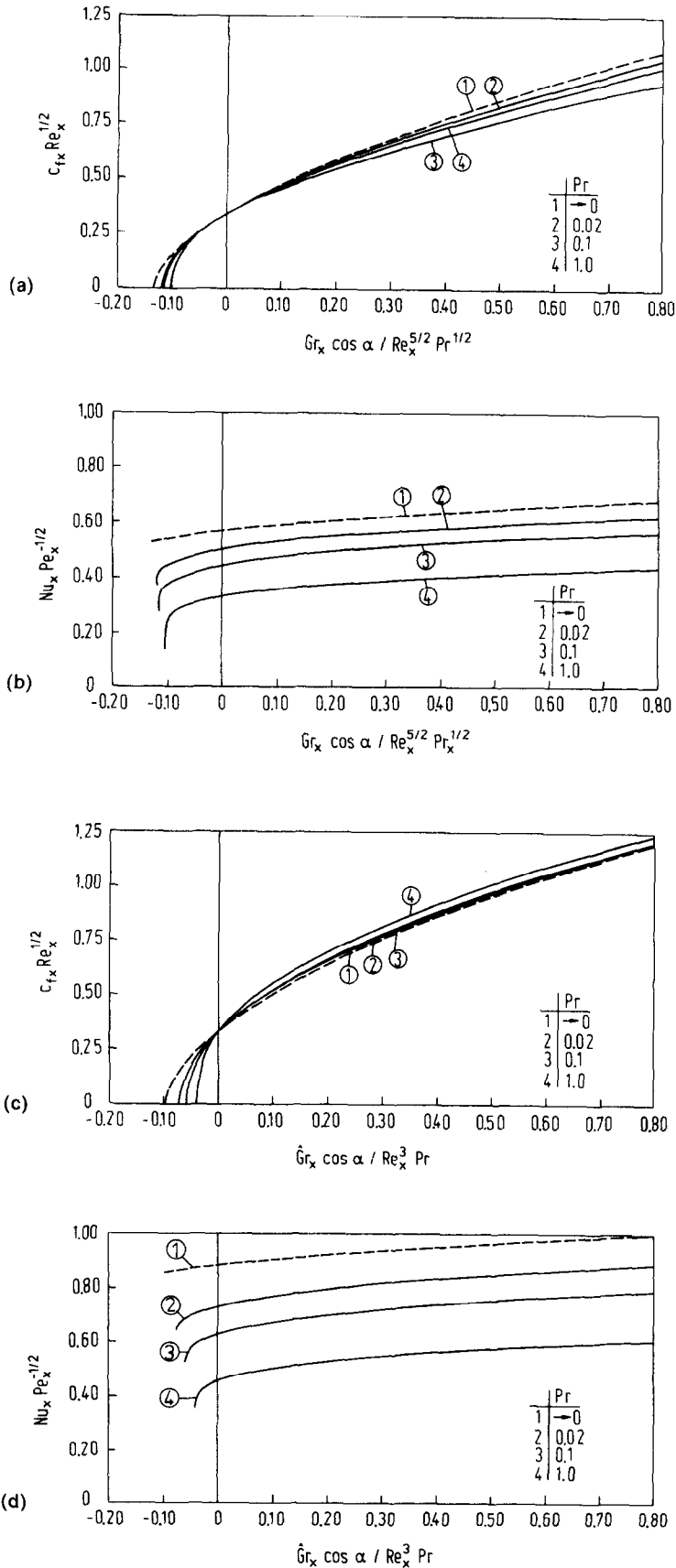


FIG. 4. Friction coefficient and Nusselt number for mixed convection from a horizontal flat plate for small Prandtl numbers: (a), (b) constant wall temperature; (c), (d) constant surface heat flux.

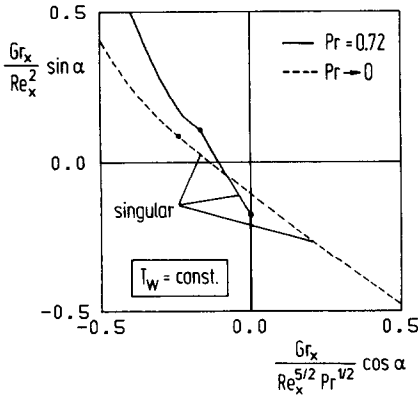


FIG. 5. Boundary of the region covered by boundary layer theory results for small Prandtl numbers.

differential equations for the inner layer are

$$\begin{aligned} \bar{f}'''' &= -x_s^{(2+2e)/(1+2e)} \frac{Gr}{Re^2} \sin \alpha \vartheta - \frac{1}{2} \bar{\eta}_T x_s \frac{Gr}{Re^{5/2}} \\ &\times \cos \alpha Pr^{-2/3} \vartheta + (\frac{1}{2} + e) x_s \frac{\partial \bar{g}}{\partial x_s} \end{aligned} \quad (24)$$

$$\bar{g}' = x_s \frac{Gr}{Re^{5/2}} \cos \alpha Pr^{-2/3} \vartheta \quad (25)$$

$$\vartheta'' + \frac{1}{2} \bar{f}' \vartheta' - e \bar{f}'' \vartheta = (\frac{1}{2} + e) x_s \left(\bar{f}' \frac{\partial \vartheta}{\partial x_s} - \frac{\partial \bar{f}'}{\partial x_s} \vartheta' \right) \quad (26)$$

(with $e = 0$ for $T_w = \text{const.}$ and $e = \frac{1}{2}$ for $\dot{q}_w = \text{const.}$, dots denote partial differentiation with respect to $\bar{\eta}_T$). Those for the outer layer reduce to

$$f''' + \frac{1}{2} f f'' = 0 \quad (27)$$

$$p' = 0 \quad (28)$$

$$\vartheta'' = 0 \quad (29)$$

Again the two layers are coupled by matching conditions. The boundary conditions completed by the

matching procedure are :

inner layer

$$\begin{aligned} \bar{f}_i(x_s, 0) &= 0 \\ \bar{f}'_i(x_s, 0) &= 0 \\ \bar{f}_i''(x_s, \infty) &= f''_o(x_s, 0) \\ \bar{g}_i(x_s, \infty) &= 0 \\ \vartheta_i(x_s, 0) &= 1 \quad (T_w = \text{const.}) \end{aligned}$$

or

$$\begin{aligned} \vartheta_i(0, 0) &= 1 \\ \vartheta_i(x_s, 0) &= \vartheta_i(0, 0) \end{aligned} \left. \vphantom{\begin{aligned} \vartheta_i(0, 0) &= 1 \\ \vartheta_i(x_s, 0) &= \vartheta_i(0, 0) \end{aligned}} \right\} (\dot{q}_w = \text{const.})$$

$$\vartheta_i(x_s, \infty) = \vartheta_o(x_s, 0) = 0 \quad (30)$$

outer layer

$$\begin{aligned} f_o(x_s, 0) &= 0 \quad \vartheta_o(x_s, 0) = 0 \\ f'_o(x_s, 0) &= 0 \\ f'_o(x_s, \infty) &= 1 \quad p_o(x_s, \infty) = 0. \end{aligned} \quad (31)$$

The energy equation in the outer layer only has the trivial solution which thus gives a zero boundary condition for the inner layer.

The outer layer always has the Blasius solution. The only important part of the boundary layer in the case $Pr \rightarrow \infty$ is the inner layer. The governing equations of the inner layer (equations (24)–(26) and (30)) were solved numerically applying the box method. The results are compared with those for finite Prandtl numbers in Figs. 7(a)–(d) (vertical plate) and in Figs. 8(a)–(d) (horizontal plate). For $Pr \rightarrow \infty$ the Prandtl number dependence of the buoyancy forces is rather strong, since Pr directly influences the amount of heated fluid. When all buoyancy parameters are rescaled by Pr , only minor effects are left over in the diagrams of Figs. 7 and 8. As in the limiting case $Pr \rightarrow 0$, the buoyancy forces mainly depend on the thickness of the thermal boundary layer. The higher the Prandtl number, the thinner the boundary layer and the weaker the influence of the buoyancy forces are, both in the aiding and in the opposing case.

In contrast to the low Prandtl number case, for high Prandtl numbers there always exists regular separation for aiding indirect and opposing direct free convection. As can be seen in Fig. 9, there is no singular line in the second quadrant. This is due to the fact, that separation as well as the pressure gradient normal to the wall (due to buoyancy forces) are confined to the inner layer. By interaction between these two flow properties, a momentum balance normal to the wall is possible, which keeps the solution regular at the onset of reversed flow. In the $Pr \rightarrow 0$ case both effects appear in different parts of the boundary layer and no interaction is possible.

5. CONCLUSIONS

The Prandtl number dependence of mixed convection flows at flat plates is investigated. Limiting

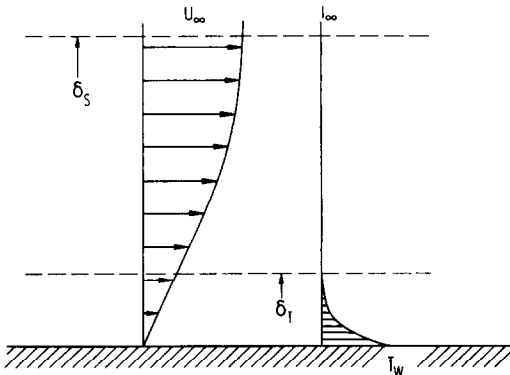


FIG. 6. Sketch of the scaling of velocity and thermal boundary layer for large Prandtl numbers.

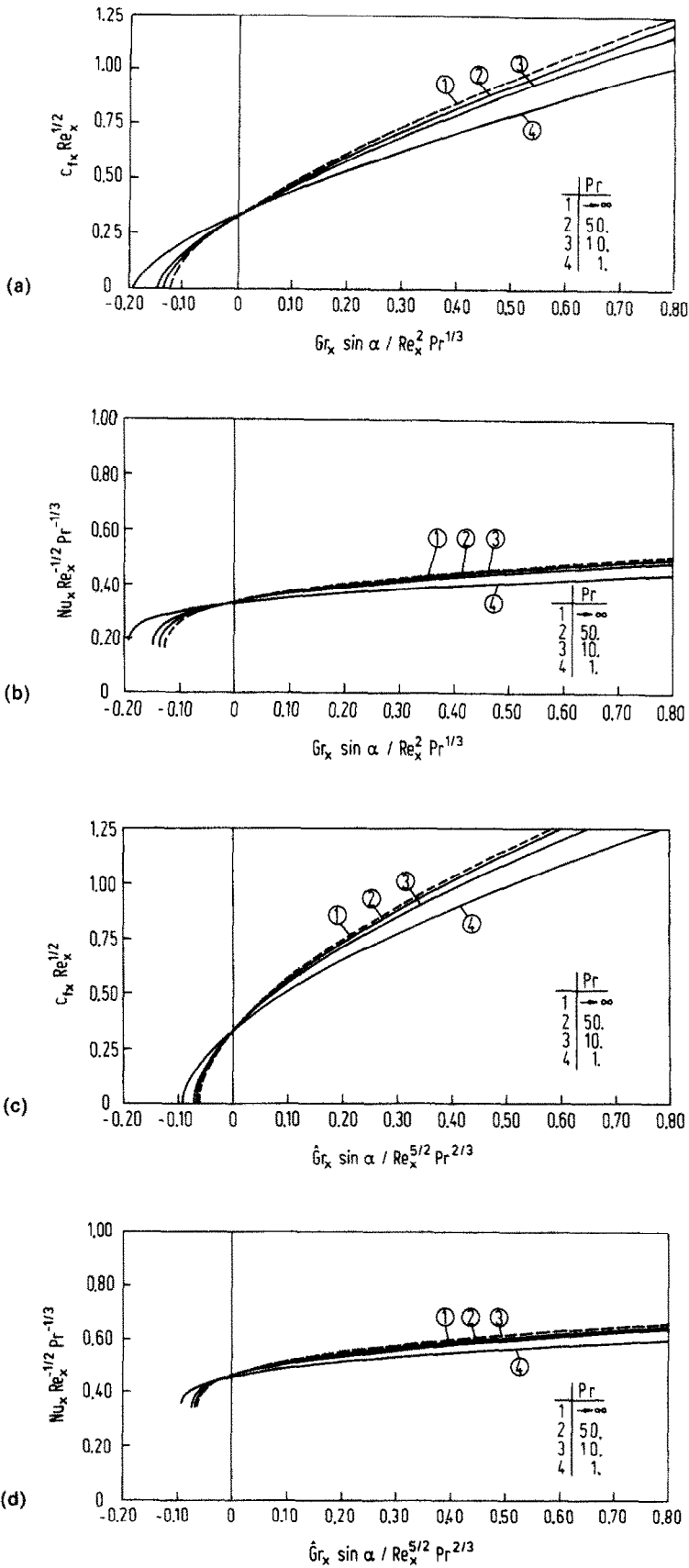


FIG. 7. Friction coefficient and Nusselt number for mixed convection from a vertical flat plate for large Prandtl numbers: (a), (b) constant wall temperature; (c), (d) constant surface heat flux.

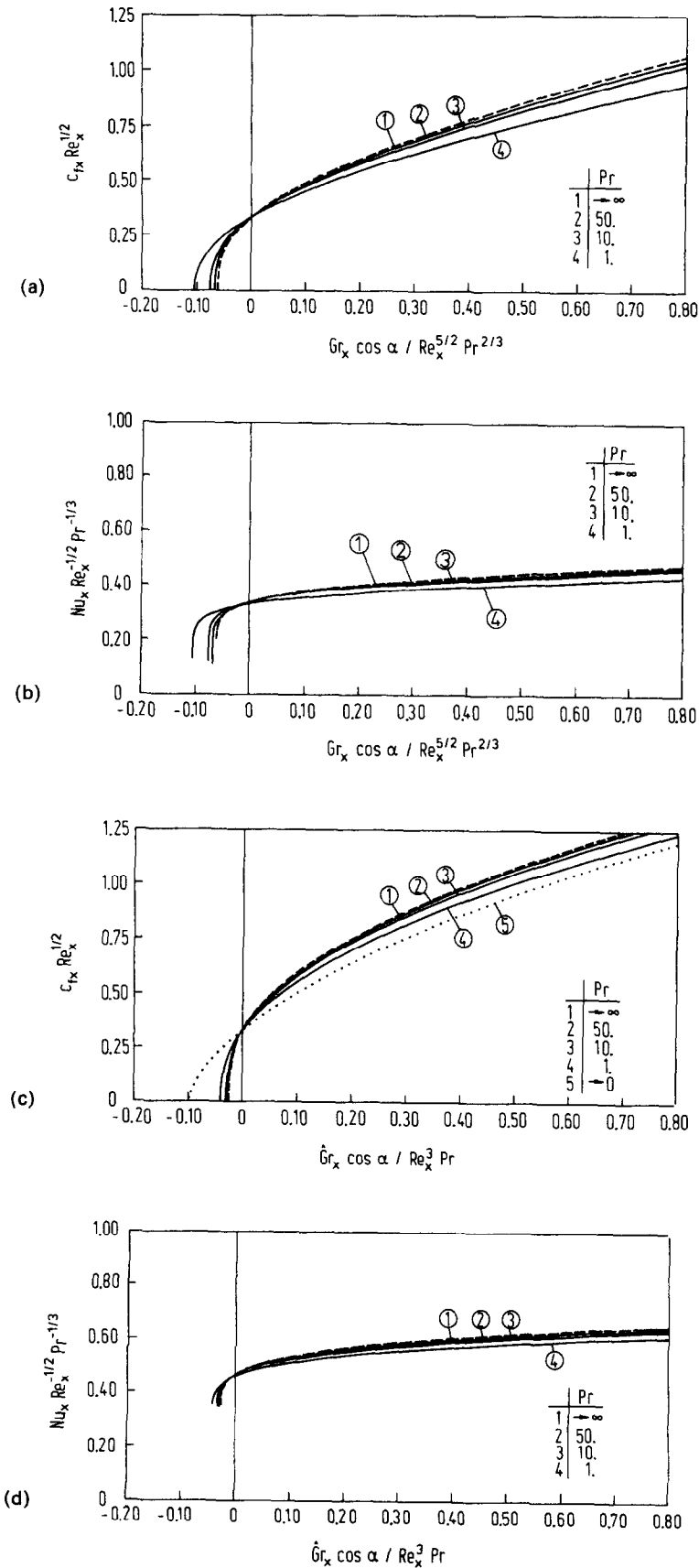


FIG. 8. Friction coefficient and Nusselt number for mixed convection from a horizontal flat plate for large Prandtl numbers: (a), (b) constant wall temperature; (c), (d) constant surface heat flux.

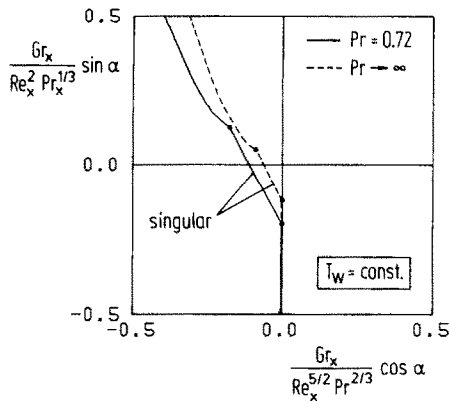


FIG. 9. Boundary of the region covered by boundary layer theory results for large Prandtl numbers.

solutions for asymptotically small and high Prandtl numbers are derived. The equations obtained are valid for arbitrarily inclined plates, though numerical results are given only for the two standard situations, i.e. vertical and horizontal plate. The thermal boundary layer scaling laws for limiting Prandtl numbers were found to be identical with those for forced convection. In addition, appropriate local buoyancy parameters (scaled with Pr) were derived. The asymptotic results are consistent with those obtained by the numerical solution for extreme but finite Prandtl numbers. Thus for purely accelerated flows a correlation formula could be found covering the whole range of Prandtl numbers and (positive) local buoyancy parameters (see Part I).

The numerical problems with separating flow encountered when calculating mixed convection from a horizontal plate with adverse buoyancy forces, reported in refs. [6, 8], were completely eliminated in the asymptotic approach $Pr \rightarrow 0$. So, this asymptotical result could be used as a reference case for modifications of the numerical scheme for finite Prandtl numbers.

On slightly inclined plates with aiding indirect free convection and adverse direct free convection in the limit $Pr \rightarrow 0$, there is a transition from regular to

singular behaviour at separation (Fig. 5). Here momentum balance in the y -direction is extremely important. For $Pr \rightarrow 0$ this balance is destroyed. A pressure gradient normal to the wall exists in the outer layer only, whereas separation occurs in the inner layer. Thus there is no interaction between boundary layer growth and pressure gradient to keep the solution regular at separation. Due to the different structure of the flow, no such singularity is encountered in the case $Pr \rightarrow \infty$ (Fig. 9).

A comprehensive discussion of the results obtained in the vicinity of the separation point will be given in a subsequent paper [9].

Acknowledgements—The author would like to thank Prof. Dr K. Gersten and Prof. Dr H. Herwig for many helpful discussions. The project was supported by the Deutsche Forschungsgemeinschaft under contract Ge 147/19-1.

REFERENCES

1. C. A. Hieber, Mixed convection above a heated horizontal surface, *Int. J. Heat Mass Transfer* **16**, 769–785 (1973).
2. T. S. Chen, E. M. Sparrow and A. Mucoglu, Mixed convection in boundary layer flow on a horizontal plate, *J. Fluid Mech.* **99**, 66–71 (1977).
3. A. Mucoglu and T. S. Chen, Mixed convection on inclined surfaces, *J. Heat Transfer* **101**, 422–426 (1979).
4. M. S. Raju, X. Q. Liu and L. K. Law, A formulation of combined forced and free convection past horizontal and vertical surfaces, *Int. J. Heat Mass Transfer* **27**, 2215–2224 (1984).
5. N. Ramachandran, B. F. Armaly and T. S. Chen, Mixed convection over a horizontal plate, *J. Heat Transfer* **105**, 420–432 (1983).
6. W. Schneider and M. G. Wasel, Breakdown of the boundary layer approximation for mixed convection above a horizontal plate, *Int. J. Heat Mass Transfer* **28**, 2307–2313 (1985).
7. S. W. Churchill and R. Usagi, A general expression for the correlation of rates of transfer and other phenomena, *A.I.Ch.E. JI* **18**, 1121–1128 (1972).
8. G. Wickern, Untersuchung der laminaren gemischten Konvektion an einer beliebig geneigten ebenen Platte mit besonderer Berücksichtigung der Strömungsablösung, *Fortschr.-Ber. VDI* **7**(129) (1987).
9. G. Wickern, Asymptotic description of separation regions in a class of mixed convection flow. To appear.

CONVECTION MIXTE SUR UNE PLAQUE PLANE, SEMI-INFINIE, INCLINEE—II. INFLUENCE DU NOMBRE DE PRANDTL

Résumé—On étudie l'effet du nombre de Prandtl sur la couche limite laminaire sur une plaque plane, semi-infinie, inclinée, chauffée ou refroidie. On détermine l'interaction entre les forces de flottement et celles de l'écoulement forcée. L'effet de l'angle d'inclinaison a été discuté dans la partie I. L'étude des plaques horizontale et verticale fournit une information suffisante pour comprendre l'écoulement sur une plaque inclinée quelconque. Ici l'influence du nombre de Prandtl est montrée seulement pour les plaques horizontale et verticale. La dépendance de l'écoulement vis-à-vis du nombre de Prandtl et celle des caractéristiques de transfert thermique est d'abord considérée de façon asymptotique pour $Pr \rightarrow 0$ et $Pr \rightarrow \infty$. En outre des solutions numériques sont données pour une variété de nombres de Prandtl. Les résultats sont comparés avec ceux de la théorie asymptotique.

GEMISCHTE KONVEKTION AN EINER BELIEBIG GENEIGTEN HALBUNENDLICHEN PLATTE—II. DER EINFLUß DER PRANDTL-ZAHL

Zusammenfassung—Der Einfluß der Prandtl-Zahl auf die laminare Grenzschichtströmung an einer beliebig geneigten halb-unendlichen ebenen Platte, die entweder geheizt oder gekühlt ist, wird untersucht. Die Wechselwirkung zwischen den Auftriebskräften und der ursprünglichen erzwungenen Konvektion wird bestimmt. Der Einfluß des Anstellwinkels wurde bereits in Teil I dargelegt. Es zeigte sich, daß eine Beschränkung auf die horizontale und vertikale Platte hinreichende Information liefert, um die Strömung an beliebig geneigten Platten zu verstehen. Die Wirkung der Prandtl-Zahl wird daher in diesem Teil hauptsächlich anhand dieser beiden Sonderfälle demonstriert. Die Prandtl-Zahl-Abhängigkeit der Strömungs- und Wärmeübergangsparameter wird zunächst mit Hilfe von asymptotischen Entwicklungen für $Pr \rightarrow 0$ und $Pr \rightarrow \infty$ untersucht. Zusätzlich werden numerische Lösungen für eine Anzahl von endlichen Prandtl-Zahlen angegeben. Die Ergebnisse werden mit der asymptotischen Theorie verglichen.

СМЕШАННАЯ КОНВЕКЦИЯ ОТ ПОЛУБЕСКОНЕЧНОЙ ПЛОСКОЙ ПЛАСТИНЫ С ПРОИЗВОЛЬНЫМ УГЛОМ НАКЛОНА—II. ЭФФЕКТ ЧИСЛА ПРАНДТЛЯ

Аннотация—Исследуется влияние числа Прандтля на ламинарное течение в пограничном слое над полубесконечной плоской пластиной с произвольным углом наклона, которая либо нагревается, либо охлаждается. Устанавливается взаимодействие между подъемными силами и основным течением, обусловленным вынужденной конвекцией. Эффект угла наклона уже обсуждался в I-й части статьи. Оказалось, что исследование соответственно горизонтальной и вертикальной пластин обеспечивает достаточное количество данных для понимания механизма течения при произвольных углах наклона пластины. Во II-й части статьи на большом количестве примеров демонстрируется эффект числа Прандтля только для горизонтальной и вертикальной пластин. Зависимость характеристик течения и теплопереноса от числа Прандтля сначала исследуется методом асимптотических разложений при $Pr \rightarrow 0$ и $Pr \rightarrow \infty$. Приводятся также численные решения для конечных чисел Прандтля. Результаты проведенного исследования сравниваются с полученными на основе асимптотической теории.